

# Site-Dilution-Induced Antiferromagnetic Long-Range Order in Two-Dimensional Spin-Gapped Heisenberg Antiferromagnet

Chitoshi Yasuda, Synge Todo\*, Munehisa Matsumoto, and Hajime Takayama  
*Institute for Solid State Physics, University of Tokyo, Kashiwa 277-8581, Japan*  
 (October 31, 2018)

Effects of the site dilution on spin-gapped Heisenberg antiferromagnets with  $S = 1/2$  and  $S = 1$  on a square lattice are investigated by means of the quantum Monte Carlo method. It is found that effective magnetic moments induced around the diluted sites exhibit the antiferromagnetic long-range order in the medium of spin-singlet pairs. Their microscopic structure is examined in detail and important roles of the higher dimensionality than one on the phenomenon are discussed.

PACS numbers: 75.10.Jm, 75.10.Nr, 75.40.Cx, 75.40.Mg

The nonmagnetic-impurity-induced, or more specifically, the site-dilution-induced antiferromagnetic long-range order (AF-LRO) in quasi-one-dimensional (Q1D) quantum antiferromagnets has attracted many researchers more than a decade [1]. Typically it has been observed in the first inorganic spin-Peierls (SP) compound  $\text{CuGeO}_3$  [2] by the substitution of nonmagnetic Zn for magnetic Cu with  $S = 1/2$  spin. In the induced AF state with sufficiently weak dilution the lattice dimerization is preserved [3]. This strongly suggests that at least this site-dilution-induced transition is dominantly of a magnetic origin, though for thorough understanding of the SP transition in the system other ingredients such as the magneto-elastic effect [4] is indispensable. Another example of the site-dilution-induced AF-LRO has been observed in a Q1D Haldane compound  $\text{Pb}(\text{Ni}_{1-x}\text{Mg}_x)_2\text{V}_2\text{O}_8$  where Ni carries  $S = 1$  spin [5].

A most plausible scenario for the site-dilution-induced AF-LRO so far discussed is as follows [1,6–9]. The mother compound ( $x = 0$ ) has a spin-gapped ground state such as the dimer singlet state in  $\text{CuGeO}_3$  and the Haldane state in  $\text{PbNi}_2\text{V}_2\text{O}_8$ . When  $x > 0$ , spins on the sites neighboring the diluted sites organize a spin cluster which is a close resemblance of the edge state in the Haldane chain [10]. Here we call it as a whole an ‘*effective spin*’. Between the effective spins there exist the effective interactions mediated by spins which are in the singlet state. The averaged magnitude of the effective interactions is exponentially small as a function of the concentration of nonmagnetic impurities. Although they are either ferromagnetic or AF depending on relative positions of the effective spins, the staggered nature with respect to the original lattice is completely preserved, and so the effective spins are antiferromagnetically ordered at  $T = 0$  in more than two dimensions. The very last part of the above scenario, i.e., the effect of the higher dimensionality, has been mostly treated by the mean-field-like arguments except for a few works [8,9].

In the present work we have extensively performed the quantum Monte Carlo (QMC) analysis on the site-diluted 2D Heisenberg antiferromagnets on a square lattice, and have reached the same scenario, but with evidences which

support it more directly than the previous works. One of them is the microscopic spatial information on the effective spins induced by the dilution. We also present the result consistent with the scenario in the 2D coupled Haldane chain system with  $S = 1$ .

The quantum spin system of our present interest is described by the Hamiltonian

$$\begin{aligned} \mathcal{H} = & \sum_{i,j} \epsilon_{2i,j} \epsilon_{2i+1,j} \mathbf{S}_{2i,j} \cdot \mathbf{S}_{2i+1,j} \\ & + \alpha \sum_{i,j} \epsilon_{2i+1,j} \epsilon_{2i+2,j} \mathbf{S}_{2i+1,j} \cdot \mathbf{S}_{2i+2,j} \\ & + J' \sum_{i,j} \epsilon_{i,j} \epsilon_{i,j+1} \mathbf{S}_{i,j} \cdot \mathbf{S}_{i,j+1}, \end{aligned} \quad (1)$$

where 1 and  $\alpha$  ( $0 \leq \alpha \leq 1$ ) are the intrachain alternating coupling constants,  $J'$  ( $\geq 0$ ) is the interchain AF coupling constant and  $\mathbf{S}_{i,j}$  is the quantum spin operator at site  $(i, j)$ . Randomly quenched magnetic occupation factors  $\{\epsilon_{i,j}\}$  independently take either 1 or 0 with probability  $1 - x$  and  $x$ , respectively, where  $x$  is the concentration of the diluted sites.

In the present work the QMC simulations with the continuous-imaginary-time loop algorithm [11] is carried out on the  $S = 1/2$  and  $S = 1$  systems on  $L \times L$  square lattices with the periodic boundary condition. For diluted systems with  $x > 0$  the number of samples averaged over is  $100 \sim 700$  depending on  $x$ . For each samples,  $10^4$  Monte Carlo steps (MCS) are spent for measurement after  $10^3$  MCS for thermalization. The staggered magnetization,  $M_s(x)$ , at zero temperature is evaluated by

$$M_s^2(x) = \lim_{L \rightarrow \infty} \lim_{T \rightarrow 0} \frac{3S_s(L, T, x)}{L^2}, \quad (2)$$

where

$$S_s(L, T, x) \equiv \frac{1}{L^2} \sum_{i,j} (-1)^{|r_i - r_j|} \langle S_i^z S_j^z \rangle \quad (3)$$

is the static staggered structure factor. The bracket  $\langle \dots \rangle$  in Eq.(3) denotes both the thermal and random averages. The value of  $S_s(L, T, x)$  converges to its zero-temperature

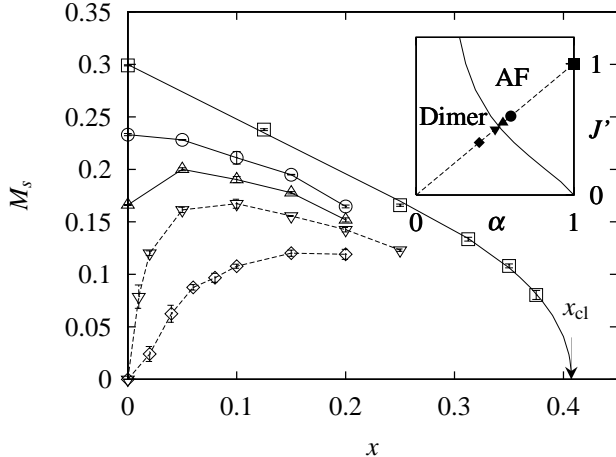


FIG. 1. Concentration dependence of the staggered magnetization at zero temperature for systems with  $\alpha = J' = 1, 0.6, 0.55, 0.5,$  and  $0.4$ . The  $\alpha - J'$  phase diagram of the pure systems is shown in the inset. The data for  $\alpha = J' = 1$  are results in ref. [13] with  $x_{cl} (\simeq 0.407254)$  being the percolation threshold. All the lines are guides to eyes.

value at  $T$  lower than either a gap due to the finiteness of the system or the intrinsic spin gap. Thus  $S_s(L, T, x)$  at low temperatures where its  $T$ -dependence becomes not discernible within the error bars is taken as an estimate of  $S_s(L, 0, x)$ .

First we determine the ground-state phase diagram of the pure systems on the  $\alpha - J'$  plane. Its details will be discussed elsewhere [12]. Here we simply show the result for the  $S = 1/2$  system in the inset of Fig. 1, and mention that, except for the critical point  $(\alpha, J') = (1, 0)$ , the quantum dimer-AF transition we obtain is ascertained to belong to the same universality class as that of the 3D classical Heisenberg model.

Now let us concentrate on the site-dilution-induced AF-LRO in the  $S = 1/2$  systems with  $\alpha = J'$  indicated in the inset of Fig. 1. Expecting that the fundamental aspects of the phenomenon do not crucially depend on the values of  $\alpha$  and  $J'$ , we choose those on the line  $\alpha = J'$ . It connects the system with  $\alpha = J' = 0$ , which consists of a set of independent dimers, and the isotropic antiferromagnet with  $\alpha = J' = 1$ . Along this line, the quantum dimer-AF phase transition occurs at  $\alpha = \alpha_c = 0.52337(3)$  [12]. The dilution effects on the isotropic system was investigated in details in the previous works [13,14]; as shown in Fig. 1, the site-dilution simply reduces  $M_s$  which exists already in the pure system. For the systems with  $\alpha = J' = 0.5$  and  $0.4$ , on the other hand,  $M_s$ , which is zero for  $x = 0$ , becomes finite even with 1 or 2 % of site dilution. This is nothing but the site-dilution-induced AF-LRO of our present interest.

The values of  $M_s$  in Fig. 1 are extracted from the  $L$ -dependence of  $S_s(L, 0, x)/L^2$  as shown in Fig. 2. The data for  $x = 0$  are well fitted to  $S_s(L, 0, x)/L^2 \propto (1 - \exp(-L/\xi_p))/L^2$ , where  $\xi_p$  is the correlation length.

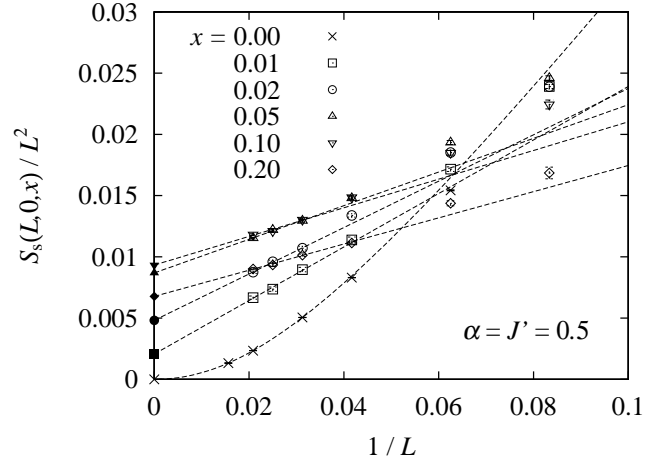


FIG. 2. System-size dependence of  $S_s(L, 0, x)/L^2$  in the case of  $\alpha = J' = 0.5$ . Dashed lines are obtained by the least-squares fitting for the largest three system sizes for each  $x$ . The extrapolated values are denoted by solid symbols.

This form is derived by the modified spin-wave theory for a spin-gapped state. For diluted systems with  $x > 0$ , on the other hand,  $M_s$  is evaluated by fitting the data to  $S_s(L, 0, x)/L^2 \simeq M_s^2/3 + a/L$  which is obtained, for example, by the linear spin-wave theory on the state with a finite  $M_s$ .

The above-mentioned correlation length of the pure system,  $\xi_p$ , is given by  $\xi_p = (\xi_p^x \xi_p^y)^{1/2}$  where  $\xi_p^x$  and  $\xi_p^y$  are the anisotropic correlation lengths. They are estimated from the dynamic staggered correlation function by using the second moment method. Similarly the spin gap,  $\Delta_p$ , is evaluated from behavior of the function on the imaginary-time axis. We obtain [12]  $\xi_p^x = 3.0089(9)$ ,  $\xi_p^y = 2.2097(6)$  and  $\Delta_p = 0.32255(3)$  for  $\alpha = J' = 0.4$  and  $\xi_p^x = 11.998(9)$ ,  $\xi_p^y = 9.312(10)$  and  $\Delta_p = 0.0918(1)$  for  $\alpha = J' = 0.5$ . The nearer to the transition point a system is, the smaller is  $\Delta_p$  and the larger is  $\xi_p$ .

In order to gain insights into nature of the site-dilution-induced AF-LRO obtained above, we investigate the local static staggered structure factor defined by

$$\mathcal{S}(i) \equiv \sum_j (-1)^{|r_i - r_j|} \langle S_i^z S_j^z \rangle. \quad (4)$$

Figure 3 shows the real-space distribution of  $\mathcal{S}(i)$  for  $\alpha = J' = 0.5$  on a  $64 \times 64$  lattice from which 30 spins are randomly removed. The temperature,  $T = 0.001$ , can be regarded as zero temperature for the system with these parameters. The points protruding downwards to zero are on the diluted sites. The peaks of  $\mathcal{S}(i)$  appear on the sites connected by a strong bond 1 with these diluted sites. Naturally they are considered to be the contribution of the spins which get rid of the singlet pairing by the dilution. The peaks exhibit a significant spatial extent whose size is given by  $\xi_p^x$  and  $\xi_p^y$  evaluated above.

From the analogy of the 1D spin-gapped state [6], the exchange coupling between the two effective spins cen-

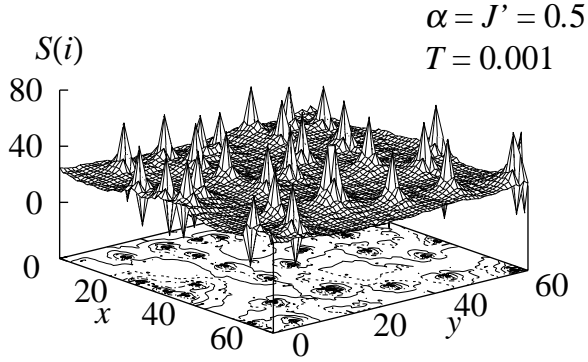


FIG. 3. 3D plot of the local static staggered structure factor in the fixed configuration of 30 impurities on a  $64 \times 64$  lattice for  $\alpha = J' = 0.5$  at  $T = 0.001$ . Contours are shown in the bottom.

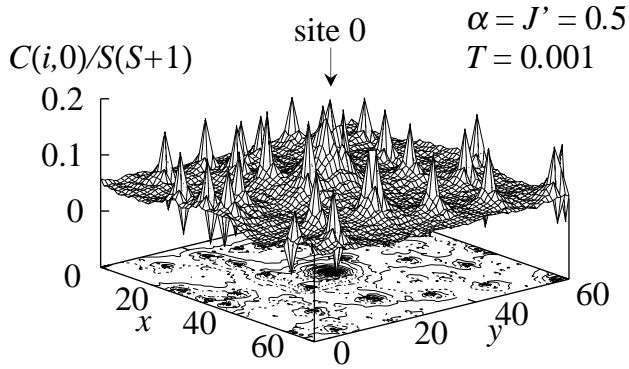


FIG. 4. 3D plot of the staggered correlation function from the peak of an induced magnetic moment on site 0 ( $= (31,31)$ ) for the same dilution configuration as Fig. 3.

tered at sites  $m$  and  $n$  is expected to be given by  $\tilde{J}_{mn} \propto (-1)^{|r_m - r_n + 1|} \exp[-l(\xi_p^x \xi_p^y)^{-1/2}]$ , where  $l = |r_m - r_n|$  is the distance between the effective spins. For a sufficiently weak dilution, we can naturally expect that the effective Hamiltonian,  $\mathcal{H}_{\text{eff}} = \sum_{\langle mn \rangle} \tilde{J}_{mn} \tilde{\mathbf{S}}_m \cdot \tilde{\mathbf{S}}_n$  well describes magnetic behavior associated with the site-dilution-induced AF-LRO. As we have already pointed out,  $\tilde{J}_{mn}$  is considered to completely preserve the staggered nature with respect to the original lattice since the original interactions are all AF with no frustration at all. This is in fact confirmed by Fig. 4 where we draw the static staggered correlation function  $C(i,0) = (-1)^{|r_i - r_0|} \langle S_i^z S_0^z \rangle$  with site 0 ( $= (31,31)$ ) being the peak position of an effective spin. The system is the same as that in Fig. 3. At any site  $i$ ,  $C(i,0)$  is positive except for the diluted sites where it is zero. It peaks at sites of other effective spins with heights almost independent of the distance from site 0, while it stays at a relatively lower value on the sites far from the diluted sites where spins form the singlet state. Thus Fig. 4 combined with

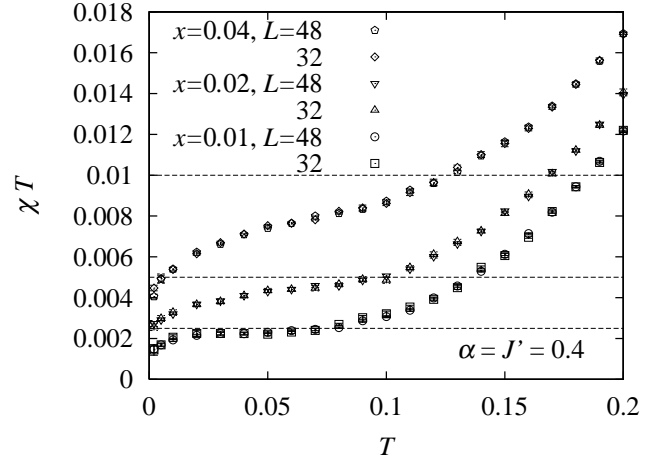


FIG. 5. Temperature dependence of the effective Curie constant for  $\alpha = J' = 0.4$ . The broken lines show  $\chi T = x/4$  for  $x = 0.04, 0.02,$  and  $0.01$  from top.

Fig. 3 clearly demonstrates that the site-dilution-induced AF-LRO is mostly carried by the effective spins. Each of them contributes to  $M_s$  by the amount proportional to  $\xi_p^2$ . This explains a sharper rise near  $x \simeq 0$  of  $M_s$  of  $\alpha = J' = 0.5$  than that of  $\alpha = J' = 0.4$  in Fig. 1. It contributes to the uniform susceptibility, on the other hand, by the amount  $|\tilde{\mathbf{S}}_m| = 1/2$  [6] as discussed below.

The averaged distance  $\langle l \rangle$  between diluted sites is proportional to  $1/\sqrt{x}$ . The typical coupling which scales the excitation energy of the spin-wave-like modes is then given by  $\langle |\tilde{J}_{mn}| \rangle \propto \exp(-1/\sqrt{x \xi_p^x \xi_p^y})$ . It becomes much smaller than  $\Delta_p$  for a sufficiently small value of  $x$ . Thus we can naturally expect the existence of low-lying excitation modes well separated from the original triplet excited state with  $\Delta_p$  as has been in fact observed by the neutron inelastic experiment in the doped  $\text{CuGeO}_3$  [3,15,16]. Another peculiar feature of the present site-dilution-induced AF-LRO is that it is inhomogeneous in a shorter length scale than  $\langle l \rangle$ . This may explain the experimental fact [3] that the spectrum of the spin-wave-like mode becomes broader for the larger wave number.

By the present simulation the existence of low-lying excitation modes mentioned above is ascertained by the  $T$ -dependence of the effective Curie constant  $\chi T$  [9] which is shown in Fig. 5 for  $\alpha = J' = 0.4$ . For  $x = 0.01$  the plateau of a height nearly equal to  $\chi T = x/4$  in unit of  $g^2 \mu_B^2 / k_B$  is clearly seen around  $T \sim 0.05$  which is smaller than  $\Delta_p$  by an order of magnitude. We can attribute the plateau to the Curie law of the effective spins with  $|\tilde{\mathbf{S}}_m| = 1/2$  as mentioned above. They start to correlate at lower temperatures than  $\langle |\tilde{J}_{mn}| \rangle$ . Already for  $x = 0.02$ , however, the plateau is obscured, indicating that  $\langle |\tilde{J}_{mn}| \rangle$  becomes comparable in magnitude with  $\Delta_p$ . Qualitatively similar features have been observed experimentally [17].

Essentially the same scenario as the  $S = 1/2$  case is

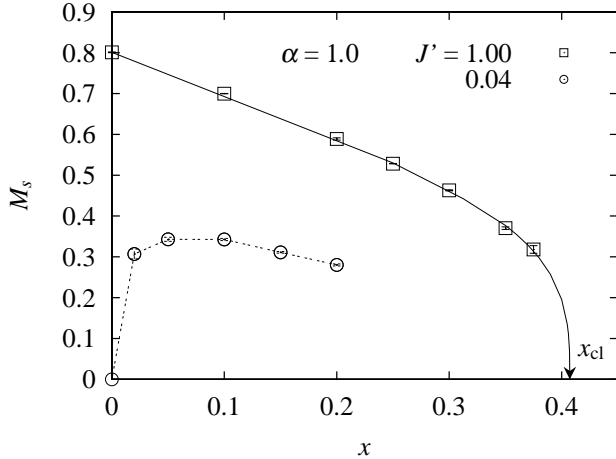


FIG. 6. The staggered magnetization of the coupled Haldane chain systems with  $J' = 1$  and  $0.04$ . The data for  $\alpha = J' = 1$  are results in ref. [13]. All the lines are guides to eyes.

expected to hold also for similar antiferromagnets with  $S = 1$ . As their representative we have examined the coupled Haldane chain system with  $\alpha = 1$  and  $J' = 0.04$  in Eq.(1). The latter is a little smaller than the critical value  $J'_c = 0.04365(1)$  for the Haldane-AF transition point [12]. Behavior of its  $M_s(x)$  shown in Fig. 6 is quite similar to that in Fig. 1, and further confirms the above-mentioned scenario for the site-dilution-induced AF-LRO.

Here it is worth noting that the interchain interaction  $J'$  introduces another energy scale than  $\Delta_p$  and  $\langle |\tilde{J}_{mn}| \rangle$  into the problem of the present interest. It is the coupling strength,  $\mathcal{J}$ , of spins on the two opposite neighbors of the diluted site through the shortest interaction paths. It is *ferromagnetic* and of the order of  $J'^2$ . For a sufficiently small  $x$ ,  $\langle |\tilde{J}_{mn}| \rangle \ll \mathcal{J} \ll \Delta_p$  holds. In such a coupled Haldane chain system the following successive process is expected to occur; effective spins with  $S = 1/2$ , instead of  $S = 1$ , induced at both sides of diluted sites are independently fluctuating at  $\mathcal{J} \ll T \ll \Delta_p$ , the two spins are coupled to behave as one effective spin of  $S = 1$  at  $\langle |\tilde{J}_{mn}| \rangle \ll T \ll \mathcal{J}$ , and then the  $S = 1$  effective spins begin to correlate antiferromagnetically at  $T \ll \langle |\tilde{J}_{mn}| \rangle$ . For the Haldane chain system in Fig. 6,  $\Delta_p \gg \mathcal{J} \sim 0.0016$  is satisfied. Unfortunately, however, the expected two-plateau structure in  $\chi T$  is hard to be seen, since  $\mathcal{J}$  is too small. In the  $S = 1/2$  system of Fig. 1, on the other hand,  $\mathcal{J} \sim \Delta_p$ , and there appears one plateau at  $T \ll \mathcal{J}$  as already shown in Fig. 5.

Another interesting problem on which  $\mathcal{J}$  plays an essential role is a possible difference between the AF-LRO's induced by site-dilution and bond-dilution. In the latter case the coupling  $\mathcal{J}$  between the two end spins of a diluted bond becomes *AF*. Therefore, if  $|\mathcal{J}|$  ( $\sim J'^2$ ) is significantly larger than  $\langle |\tilde{J}_{mn}| \rangle$ , the two spins may again form a singlet pair and cannot contribute to the AF-LRO. This implies a possible existence of a criti-

cal concentration  $x_c$  below which the AF-LRO does not come out. In contrast, there is no reason for a finite  $x_c$  in the site-diluted case discussed above. Experimentally, however, no drastic difference has been observed between site-diluted and bond-disordered  $\text{CuGeO}_3$  yet [16]. For quantitative understanding of the experimental results we have to take into account other ingredients than those in Eq.(1) such as the next-nearest-neighboring intra-chain interactions [18]. This is beyond the scope of the present work.

In summary, we have argued based on the QMC simulation on the 2D AF Heisenberg models that dilution of spins in a system having the spin-gapped ground state induces effective spins which are strongly correlated. As a consequence there occurs the AF-LRO state which has low-lying excitation states well separated from the original triplet excited state.

Most of numerical calculations in the present work have been performed on the SGI 2800 at Institute for Solid State Physics, University of Tokyo. The present work is supported by the ‘‘Research for the Future Program’’ (JSPS-RFTF97P01103) of Japan Society for the Promotion of Science.

- 
- \* Present address: Theoretische Physik, Eidgenössische Technische Hochschule, CH-8093 Zürich, Switzerland.
- [1] E. F. Shender and S. A. Kivelson, Phys. Rev. Lett. **66**, 2384 (1991).
  - [2] M. Hase, I. Terasaki and K. Uchinokura, Phys. Rev. Lett. **70**, 3651 (1993).
  - [3] M. C. Martin *et al.*, Phys. Rev. B **56**, 3173 (1997).
  - [4] H. Fukuyama, T. Tanomoto and M. Saito, J. Phys. Soc. Jpn. **65**, 1182 (1996).
  - [5] Y. Uchiyama *et al.*, Phys. Rev. Lett. **83**, 632 (1999).
  - [6] N. Nagaosa *et al.*, J. Phys. Soc. Jpn. **65**, 3724 (1996); Y. Iino and M. Imada, J. Phys. Soc. Jpn. **65**, 3728 (1996).
  - [7] G. B. Martins *et al.*, Phys. Rev. Lett. **78**, 3563 (1997).
  - [8] M. Imada and Y. Iino, J. Phys. Soc. Jpn. **66**, 568 (1997).
  - [9] S. Wessel *et al.*, Phys. Rev. Lett. **86**, 1086 (2001).
  - [10] S. Miyashita and S. Yamamoto, Phys. Rev. B **48**, 913 (1993).
  - [11] H. G. Evertz, G. Lana and M. Marcu, Phys. Rev. Lett. **70**, 875 (1993); B. B. Beard and U.-J. Wiese, Phys. Rev. Lett. **77**, 5130 (1996); S. Todo and K. Kato, cond-mat/9911047 (unpublished).
  - [12] M. Matsumoto *et al.*, (unpublished).
  - [13] K. Kato *et al.*, Phys. Rev. Lett. **84**, 4204 (2000).
  - [14] C. Yasuda *et al.*, Phys. Rev. B **63**, 140415(R) (2001).
  - [15] T. Masuda *et al.*, Phys. Rev. Lett. **80**, 4566 (1998).
  - [16] L. P. Regnault *et al.*, Europhys. Lett. **32**, 579 (1995).
  - [17] K. Manabe *et al.*, Phys. Rev. B **58**, R575 (1998).
  - [18] G. Castilla, S. Chakravarty and V. J. Emery, Phys. Rev. Lett. **75**, 1823 (1995).